Nonlinear polarization evolution of ultrashort pulses in microstructure fiber

T. M. Fortier and S. T. Cundiff

JILA, University of Colorado and National Institute of Standards and Technology, Boulder, Colorado 80309-0440

I. T. Lima, Jr.,* B. S. Marks, and C. R. Menyuk

Department of Computer Science and Electrical Engineering, University of Maryland, Baltimore County, 1000 Hilltop Circle, Baltimore, Maryland 21250

R. S. Windeler

OFS Fitel Laboratories, Murray Hill, New Jersey 07974

Received June 14, 2004

We present experimental and numerical results for nonlinear polarization evolution of femtosecond pulses during propagation in microstructure fiber. Numerical modeling shows that fiber dispersion permits a long interaction length between the components polarized along the two principal axes, thereby enhancing the effective nonlinear polarization evolution in microstructure fiber. © 2004 Optical Society of America

OCIS codes: 320.7140, 060.7140, 060.5530.

Microstructure (MS) fiber has the remarkable properties of low dispersion in the near infrared and very high nonlinearity, compared with ordinary fiber, due to tight confinement in a small core. This means that strong nonlinearity can be observed with nanojoule energy pulses over mere centimeter propagation distances.[1] The most dramatic example is continuum generation, which has widespread applications, ranging from optical coherence tomography[2] to optical frequency metrology.[3–5] Much effort is focused on understanding the complex interplay between nonlinearity and propagation.[6,7] Despite the experimental fact that the input polarization must be adjusted to obtain optimum continuum generation,[8] little effort has been put into understanding the polarization properties of the continuum, which have theoretically been shown to be complex.[9] Here, we present measurements and theory of the nonlinear polarization evolution in MS fiber of ultrashort pulses from a mode-locked Ti:sapphire laser. Theory shows that dispersion actually enhances the effect of nonlinearity and is required to obtain qualitative agreement with the experiment.

The MS fiber cladding consists of a honeycomb structure of airholes. Asymmetry that occurs during the pulling of the MS fiber can produce birefringence. The resulting retardance affects continuum generation, whereby optimal spectral broadening is obtained for incident light polarized along a preferred axis. Light that is injected along a primary axis of the fiber maintains its input polarization, demonstrating that the fiber does have well-defined principal axes. The strength of the linear retardance of the fiber can be easily determined by launching low-intensity, broadband linearly polarized light into the fiber at 45° to the primary axes [see Fig. 1(a)]. As shown in Fig. 1(b), by analyzing the output using a polarizer set with its polarization axis either copolarized or cross polarized with the input light, one obtains a spectral fringe pattern from which the linear retardance can be determined. This retardance measurement was performed for a 10-cm-long MS fiber[1,10] with a coupled pulse energy of 5.74 pJ. The Ti:sapphire laser operates at a center wavelength of 820 nm. The ~15-fs pulses are characterized with interferometric autocorrelation to verify that they have minimal chirp at the fiber input. Analysis of the fringe pattern yields a linear retardance $\Delta n = 2 \times 10^{-4}$, corresponding to a beat length of $z_b \simeq 0.6$ cm.[11]

Increasing the intensity causes a qualitative change in the fringe pattern, i.e., a nonlinear change in birefringence as shown in Fig. 1(c). This behavior

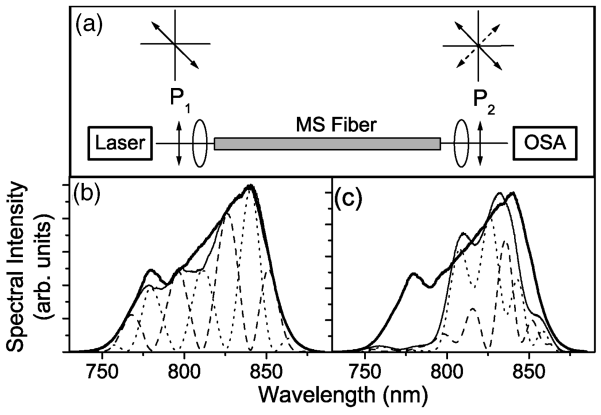

Fig. 1. (a) Schematic of experiment used to measure the retardance of MS fiber. Polarizer P_1 determines the input polarization and is set at 45° with respect to the principal axes of the fiber, whereas P_2 analyzes the output and is either copolarized with P_1 [dashed curves in (b) and (c)] or cross polarized (dotted curves). The spectra were collected with an optical spectrum analyzer (OSA). Results of the retardance measurement for a 10-cm MS fiber for (b) low (5.74-pJ) and (c) high (37-pJ) coupled pulse energy. The solid curves are the normalized spectra before the polarizer and input spectrum (bold).

0146-9592/04/212548-03$15.00/0

is caused by complex interplay between nonlinearity, linear retardance due to the birefringence-induced differential group delay, and chromatic dispersion. First, it is apparent that linear retardance by itself cannot account for the behavior. On the other hand, since self- and cross-phase modulation are initially equally balanced with the signal injected at 45° to the axes of birefringence, the group-velocity walk-off between the pulse components polarized along the two axes plays an important role in unbalancing the nonlinearity. Additionally, the apparent suppression of the spectrum below the zero-dispersion point at 770 nm is reminiscent of what occurs when solitons are injected into an optical fiber near the zero-dispersion point.[12,13]

Analysis of the nonlinear polarization evolution requires the full vector model of light propagation in the optical fiber. This propagation is accurately described by the coupled nonlinear Schrödinger equation,[11,14] which we write compactly as[15,16]

$$i\frac{\partial \mathbf{u}}{\partial z} + \frac{1}{2}\Delta\beta\sigma_3\mathbf{u} + \frac{i}{2}\Delta\beta'\sigma_3\frac{\partial \mathbf{u}}{\partial t} - \frac{1}{2}\beta''\frac{\partial^2\mathbf{u}}{\partial t^2} - \frac{i}{6}\beta'''\frac{\partial^3\mathbf{u}}{\partial t^3} + \gamma\left[|\mathbf{u}|^2\mathbf{u} - \frac{1}{3}(\mathbf{u}^\dagger\sigma_2\mathbf{u})\sigma_2\mathbf{u}\right] = 0, \quad (1)$$

where $\mathbf{u} = (u_1, u_2)^t$ is the Stokes vector of the complex wave envelopes along the fast and slow axes, z is the distance along the fiber, t is the retarded time, $\Delta\beta$ is the wave-number difference at the signal's central frequency between the fast and slow axes, and $\Delta\beta'$ is its angular frequency derivative. The dispersion is characterized by parameters β'' and β''', which are the second and third angular frequency derivatives, respectively, of the average wave number β at the central frequency. Nonlinear coefficient γ controls the self-phase modulation, cross-phase modulation, and four-wave mixing terms that appear in square brackets. We use σ_2 and σ_3 to denote the second and third Pauli matrices, and $u^\dagger$ denotes the Hermitian conjugate of u (u_1^*, u_2^*). We found that it was necessary to include third-order dispersion to obtain good qualitative agreement between theory and experiment. However, we did not find it necessary to include the Raman effect. From the core size of 1.7 μm, $\gamma = 0.047\ \mathrm{W^{-1}\ m^{-1}}$. On the basis of this measurement,[1] we assume a zero-dispersion wavelength of 770 nm and a dispersion slope of $\mathrm{d}D/\mathrm{d}\lambda = 0.34\ \mathrm{ps/nm^2/km}$, corresponding to $\beta''' = 33.2\ \mathrm{ps^3/m}$. The birefringence derived from Fig. 1(b) gives $\Delta\beta = 1827\ \mathrm{m^{-1}}$ and $\Delta\beta' = 744\ \mathrm{fs/m}$.

Figure 2 shows the theoretical simulation of the experiment for 37-pJ Gaussian pulses, both ignoring chromatic dispersion [Fig. 2(a)] and including it [Fig. 2(b)]. It is clear that, when dispersion is ignored, the results differ qualitatively from the experiment. The spectral broadening is greater in the absence of dispersion, which is indicative of greater net nonlinearity because the pulse maintains its peak power. However, the spectral fringes are still regularly spaced, as is the case at low intensity, which indicates that the nonlinearity does not affect the polarization evolution. The nonlinear polarization evolution becomes apparent when dispersion is included in the theory, and the results become qualitatively similar to the experiment. At low pulse energy the fringes are equally spaced at the same position whether or not dispersion is included.

The increased nonlinear polarization rotation in the presence of chromatic dispersion may appear counterintuitive since dispersion decreases the nonlinearity by spreading the pulses and decreasing their power. To understand the observed behavior and the regimes in which it occurs, it is useful to compare the key scale lengths. First is walk-off length $z_w = (n/\Delta n)v_g\tau \simeq 2.3$ cm, where τ is the pulse duration. Second is dispersive length $z_d = 2\tau/\beta'''\Delta\omega \simeq 1.4$ cm, where $\Delta\omega$ is the maximum frequency separation between the zero-dispersion point and a spectral component of the signal. Third is nonlinear length $z_n = (\gamma P)^{-1}$, where P is the peak power of the signal. For 5.74-pJ pulses, $z_n \simeq 2.7$ cm and $z_d < z_w < z_n$, whereas for 37-pJ pulses, $z_n < z_d < z_w$. In systems in which z_w is the shortest scale length, as occurs in the simulation for 5.74-pJ pulses when dispersion is turned off, the two polarizations separate, and their nonlinear interaction ceases. In systems in which $z_d < z_w$ the two polarizations spread and never separate. Since the power decreases approximately as $1/z$, the nonlinearity induced polarization rotation increases logarithmically over the entire length of the fiber. Additionally, when $z_n < z_w$, as occurs with 37-pJ pulses, the nonlinearity may play a role in suppressing the walk-off in analogy to soliton self-trapping.

We observed that with 5.74-pJ pulses length z_n is the longest scale length, whereas with 37-pJ pulses it is the shortest. Thus we would expect to see a transition from essentially linear behavior to behavior that is dominated by nonlinearity, as is indeed observed in both experiments and simulations. We note, however, that all scale lengths are approximately equal, which allows us to observe the interplay among the different effects but complicates the interpretation of the results.

To provide a better comparison with the experiment, we also performed the calculations with the actual experimental input spectrum and best estimates of the fiber parameters.[10] The results, shown in Fig. 3, give good qualitative agreement with the experiments. The detailed structure is sensitive to a large number of parameters of both the fiber (zero-dispersion wavelength, dispersion slope, effective nonlinearity, etc.) and the pulse (energy, chirp, etc.). When we turn

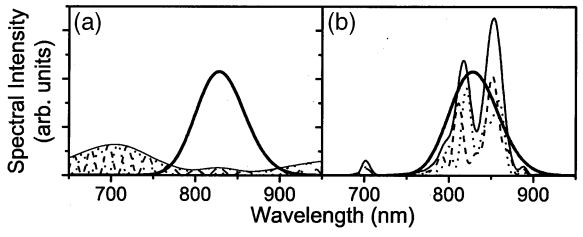

Fig. 2. Theoretical simulation for 10 cm of MS fiber and 37-pJ pulses (a) without and (b) with dispersion.

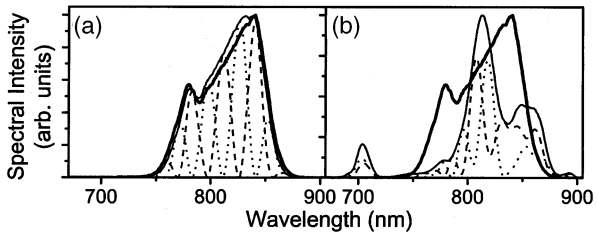

Fig. 3. Theoretical simulation using the experimental input spectrum assuming no chirp for (a) 5.74-pJ pulses and (b) 37-pJ pulses. Curves and normalization match Fig. 1.

off the terms in the complex nonlinear Schrödinger equation that couple the two components together, we see regularly spaced fringes at both powers, proving that the nonlinear interaction is responsible for our observations.

Nonlinear polarization evolution can significantly affect applications. For experiments related to carrier-envelope phase stabilization,[5] including optical frequency metrology, optical atomic clocks, and coherent control,[17] nonlinear polarization evolution can enhance the conversion of amplitude to phase noise,[18] thereby corrupting the stabilization signal. In many applications the optical elements following the continuum generation are polarization selective, which means that amplitude noise can be effectively amplified. Finally, polarization selectivity adds significant structure to the spectrum.

In summary, we have measured and modeled nonlinear polarization evolution in microstructure fiber. Comparison between measurement and theory shows that chromatic dispersion plays an important role in actually enhancing the nonlinear polarization evolution while decreasing other nonlinearities. We obtain qualitative agreement between theory and experiment for the evolution of the fringe pattern as a function of pulse energy.

The National Institute of Standards and Technology and the National Science Foundation (NSF) provided funding for the work at JILA. Work at the University of Maryland, Baltimore County, was supported by the NSF, the Department of Energy, and the National Research Laboratories. I. T. Lima, Jr., acknowledges funding from the NSF. T. M. Fortier acknowledges funding from the National Science and Engineering Council of Canada. S. T. Cundiff (e-mail cundiffs@jila.colorado.edu) is a staff member of the National Institute of Standards and Technology Quantum Physics Division.

*Present address, Department of Electrical and Computer Engineering, North Dakota State University, Fargo, North Dakota 58105-5285.

References

1. J. K. Ranka, R. S. Windeler, and A. J. Stentz, Opt. Lett. **25,** 25 (2000).
2. I. Hartl, X. D. Li, C. Chudoba, R. K. Ghanta, T. H. Ko, J. G. Fujimoto, J. K. Ranka, and R. S. Windeler, Opt. Lett. **26,** 608 (2001).
3. D. J. Jones, S. A. Diddams, J. K. Ranka, A. Stentz, R. S. Windeler, J. L. Hall, and S. T. Cundiff, Science **288,** 635 (2000).
4. A. Apolonski, A. Poppe, G. Tempea, C. Spielmann, T. Udem, R. Holzwarth, T. W. Hänsch, and F. Krausz, Phys. Rev. Lett. **85,** 740 (2000).
5. For a recent review please see S. T. Cundiff and J. Ye, Rev. Mod. Phys. **75,** 325 (2003).
6. A. L. Gaeta, Opt. Lett. **27,** 924 (2002).
7. J. Herrmann, U. Griebner, N. Zhavoronkov, A. Husakou, D. Nickel, J. C. Knight, W. J. Wadsworth, P. S. J. Russell, and G. Korn, Phys. Rev. Lett. **88,** 173901 (2002).
8. See, for example, V. L. Kalashnikov, P. Dombi, T. Fuji, W. J. Wadsworth, J. C. Knight, P. St. J. Russell, R. S. Windeler, and A. Apolonski, Appl. Phys. B **77,** 319 (2003).
9. Z. Zhu and T. G. Brown, J. Opt. Soc. Am. B **21,** 249 (2004).
10. J. K. Ranka, R. S. Windeler, and A. J. Stentz, Opt. Lett. **25,** 796 (2000).
11. G. P. Agrawal, *Nonlinear Fiber Optics*, 2nd ed. (Academic, San Diego, Calif., 1995).
12. P. K. A. Wai, C. R. Menyuk, H. H. Chen, and Y. C. Lee, Opt. Lett. **12,** 628 (1987).
13. A. S. Gouveia-Neto, M. E. Faldon, and J. R. Taylor, Opt. Lett. **13,** 770 (1988).
14. C. R. Menyuk, Opt. Lett. **12,** 614 (1987).
15. D. Marcuse, C. R. Menyuk, and P. K. A. Wai, J. Lightwave Technol. **15,** 1735 (1997).
16. C. R. Menyuk, J. Opt. Soc. Am. B **5,** 392 (1989).
17. T. M. Fortier, P. A. Roos, D. J. Jones, S. T. Cundiff, R. D. R. Bhat, and J. E. Sipe, Phys. Rev. Lett. **92,** 147403 (2004).
18. T. M. Fortier, J. Ye, S. T. Cundiff, and R. S. Windeler, Opt. Lett. **27,** 445 (2002).